# Stability And Accuracy Of a High Order Time Marching Scheme for Compressible Euler Equations

Sahar Shpitz

Advisor: Dr. Yuval Levy

# Contents

**1 Introduction** **1**

**2 Mathematical Model and Numerical Scheme** **2**

2.1 Compressible Euler Equations in One Dimension . . . . . 2

2.2 Pseudo Time Formulation . . . . . 3

2.3 Finite Volume Formulation . . . . . 4

2.3.1 Roe Flux Splitting Scheme . . . . . 5

2.3.2 Positivity Preserving Scheme (CDF+) . . . . . 5

2.3.3 Fifth Order WENO . . . . . 7

**3 Sod Test Case** **9**

**4 Conclusion** **12**

**References** **13**

# List of Figures

3.1 Density profile at $t = 0.4ms$, $\Delta t = 1$ $[\mu s]$ . . . . . 10

3.2 Temperature profile at $t = 0.4ms$, $\Delta t = 1$ $[\mu s]$ . . . . . 10

3.3 Density profile at $t = 0.4ms$, $\Delta t = 5$ $[\mu s]$ . . . . . 11

# List of Tables

3.1 Relative error of each scheme using different time steps . . . . . 11

**Abstract**

A new scheme for solving the compressible Euler equations that can be used with dual time stepping is reproduced and subsequently tested. A slight modification to the eigenvectors of the Jacobian matrix produces a scheme that is positivity preserving and monotone near discontinues. The new scheme is superior to standard second order backward difference schemes so that a larger time step can be used without loss of accuracy, stability, or monotonicity. A Sod test case confirms the stability and accuracy of the scheme.

# Chapter 1

# Introduction

Dual time stepping is a technique that is used to obtain accurate unsteady solutions for hyperbolic PDEs. The basic idea is to add an artificial, pseudo-time derivative, to the original equation and use sub iterations until the residual ,which consists of the sum of original time and space derivatives, drops to zero. At that stage, the pseudo-time scheme has reached convergence and therefore the unsteady solution has been found. Using dual-time stepping allows to use high order temporal derivatives and to use a relatively large time steps, thus increasing both computational accuracy and efficiency.

However, the use of high order backward difference formulae (BDF) for the temporal derivative can often induce non-physical oscillations at discontinuities (*e.g.*, shock-waves) leading to inaccurate solutions and converges difficulties. In addition, the use of high order BDF schemes is not positivity preserving, meaning that the primitive variables, *e.g.* the pressure, density, and temperature can become negative, which are nonphysical. Using first a order approximation for the temporal derivative is a monotonicity and positivity preserving scheme but it is considered dissipative and therefore it is desired to be able to use higher order schemes.

To overcome the deficiencies of existing finite difference stencils, a new approach has been proposed for discretizing the temporal derivative within the dual-time stepping framework [5]. This approach follows the Cauchy–Kowalevski procedure, leading to cross differences in space-time, but with several novel modifications that guarantee that the resulting discretized equation in space-time has all-positive coefficients. Not only does this lead to a monotone solution that is free of spurious oscillations near discontinuities, but this also leads to a high order, efficient and positivity-preserving scheme.

# Chapter 2

# Mathematical Model and Numerical Scheme

## 2.1 Compressible Euler Equations in One Dimension

The 1-D inviscid compressible Euler equations are given by

$$\frac{\partial Q}{\partial t} + \frac{\partial E}{\partial x} = 0 \tag{2.1.1}$$

where $Q$ is the vector of flow variables, namely,

$$Q = \begin{bmatrix} \rho \\ \rho u \\ e \end{bmatrix} \tag{2.1.2}$$

where $\rho$ is the fluid density, $u$ is the velocity, and $e$ the total energy per unit volume. The vector $E$ is the convective flux vector, given by

$$E = \begin{bmatrix} \rho u \\ \rho u^2 + p \\ (e+p)u \end{bmatrix} \tag{2.1.3}$$

where $p$ is the pressure. For a calorically perfect gas the energy and pressure are related by the equation of state

$$e = \frac{p}{\gamma - 1} + \frac{1}{2}\rho u^2 \tag{2.1.4}$$

where $\gamma$ is the heat capacity ratio. Equation (2.1.1) can be rewritten in a quasi linear form

$$\frac{\partial Q}{\partial t} + A\frac{\partial Q}{\partial x} = 0 \tag{2.1.5}$$

The matrix $A$ is the flux jacobian matrix and is given by

$$A = \frac{\partial E}{\partial Q} = \begin{bmatrix} 0 & 1 & 0 \\ \frac{1}{2}u^2 & (3-\gamma)u & \gamma - 1 \\ u\left[\frac{1}{2}(\gamma-1)u^2 - H\right] & H - (\gamma-1)u^2 & \gamma u \end{bmatrix} \tag{2.1.6}$$

where $H$ is the enthalpy, defined by

$$H = \frac{e+p}{\rho} \tag{2.1.7}$$

The flux Jacobian can be expressed in terms of the eigenvalues and eigenvectors by the following diagonal decomposition

$$A = T\Lambda T^{-1} \tag{2.1.8}$$

where $\Lambda$ is a diagonal matrix formed from the eigenvalues of $A$ and the columns of $T$ are the corresponding eigenvectors of $A$. The matrices are given by

$$\Lambda = \begin{bmatrix} u-a & 0 & 0 \\ 0 & u & 0 \\ 0 & 0 & u+a \end{bmatrix} \tag{2.1.9}$$

$$T = \begin{bmatrix} 1 & 1 & 1 \\ u-a & u & u+a \\ H-ua & \frac{1}{2}u^2 & H+ua \end{bmatrix} \tag{2.1.10}$$

$$T^{-1} = \begin{bmatrix} \frac{\gamma-1}{4}\frac{u^2}{a^2} + \frac{u}{2a} & -\frac{\gamma-1}{2}\frac{u}{a^2} - \frac{1}{2a} & \frac{\gamma-1}{2a^2} \\ 1 - \frac{\gamma-1}{2}\frac{u^2}{a^2} & (\gamma-1)\frac{u}{a^2} & -\frac{\gamma-1}{a^2} \\ \frac{\gamma-1}{4}\frac{u^2}{a^2} - \frac{u}{2a} & -\frac{\gamma-1}{2}\frac{u}{a^2} + \frac{1}{2a} & \frac{\gamma-1}{2a^2} \end{bmatrix} \tag{2.1.11}$$

where $a = \sqrt{\frac{\gamma p}{\rho}}$ is the speed of sound.

## 2.2 Pseudo Time Formulation

As outlined by Ferziger and Perio [2], dual time stepping is a method that's used to obtain an accurate solution for unsteady flows. A pseudo time derivative is added to Equation (2.1.1)

$$\frac{\partial Q}{\partial \tau} + \frac{\partial Q}{\partial t} + \frac{\partial E}{\partial x} = 0 \tag{2.2.1}$$

where $\tau$ is the pseudo time. For a fixed physical time $t$ reaching a pseudo steady state, namely $\frac{\partial Q}{\partial \tau} \to 0$ clearly satisfies the original equation. The introduction of the pseudo time derivative allows for the use of time marching schemes that are used to solve hyperbolic PDEs in order to obtain the accurate unsteady solution at every physical time.

## 2.3 Finite Volume Formulation

A finite volume scheme may be realized by defining:

$$R_i = \frac{\partial E_i}{\partial x} = \frac{1}{\Delta x}\left(E_{i+\frac{1}{2}} - E_{i-\frac{1}{2}}\right) \tag{2.3.1}$$

An implicit, temporally first order scheme may be realized by using two point backward differences for the time derivative (the BDF1 scheme). By applying the BDF1 scheme Equation (2.2.1) becomes

$$\frac{Q_i^{k+1} - Q_i^k}{\Delta \tau} + \frac{Q_i^{k+1} - Q_i^n}{\Delta t} + R_i^{k+1} = 0 \tag{2.3.2}$$

where $t$ and $n$ are the physical time and the physical time step, respectively, and $\tau$ and $k$ are the pseudo time and the pseudo time step, respectively.

For every fixed physical time level $n+1$ the pseudo time is iterated until reaching convergence, in the pseudo time sense, namely:

$$Q^{k+1} = Q^k = Q^{n+1} \tag{2.3.3}$$

Using a first order Tylor series expansion, Equation (2.3.1) becomes

$$R_i^{k+1} \approx R_i^k + \frac{\partial R_i^k}{\partial Q}\Delta Q^k = R_i^k + \frac{\partial R_i^k}{\partial Q_{i-1}}\Delta Q_{i-1}^k + \frac{\partial R_i^k}{\partial Qi}\Delta Q_i^k + \frac{\partial R_i^k}{\partial Q_{i+1}}\Delta Q_{i+1}^k \tag{2.3.4}$$

Substituting Equation (2.3.4) into Equation (2.3.2) and rearranging the terms yields the following finite difference formulation:

$$\frac{\partial R_i^k}{\partial Q_{i-1}}\Delta Q_{i-1}^k + \left(\frac{1}{\Delta \tau} + \frac{1}{\Delta t} + \frac{\partial R_i^k}{\partial Qi}\right)\Delta Q_i^k + \frac{\partial R_i^k}{\partial Q_{i+1}}\Delta Q_{i+1}^k = -R_i^k + \frac{Q_i^n - Q_i^k}{\Delta t} \tag{2.3.5}$$

where

$$\Delta Q^k = Q^{k+1} - Q^k \tag{2.3.6}$$

Equation (2.3.5) represents a block tridiagonal system of equations which may be solved using a tridiagonal matrix solver algorithm.

Similarly, a second order in time implicit scheme may be written by using a three point backward difference operator for the time derivative (the BDF2 scheme), namely,

$$\frac{Q_i^{k+1} - Q_i^k}{\Delta \tau} + \frac{3Q_i^{k+1} - 4Q_i^n + Q_i^{n-1}}{2\Delta t} + R_i^{k+1} = 0 \tag{2.3.7}$$

A similar manipulation to that applied for the BFD1 scheme yields

$$\frac{\partial R_i^k}{\partial Q_{i-1}}\Delta Q_{i-1}^k + \left(\frac{1}{\Delta \tau} + \frac{3}{2\Delta t} + \frac{\partial R_i^k}{\partial Qi}\right)\Delta Q_i^k + \frac{\partial R_i^k}{\partial Q_{i+1}}\Delta Q_{i+1}^k = -R_i^k - \frac{3Q_i^k - 4Q_i^n + Q_i^{n-1}}{2\Delta t} \tag{2.3.8}$$

Using the BDF2 scheme requires a single step scheme for the first step. One could use the BDF1 scheme or a single step second order scheme.

### 2.3.1 Roe Flux Splitting Scheme

The Roe scheme is a flux difference splitting scheme (FDS scheme). The scheme splits the fluxes based on the approximate solution of a local Riemann problem [6]. The numerical flux at the cell interface according to the Roe scheme is given by

$$E_{i+\frac{1}{2}} = \frac{1}{2}\left[(E_L + E_R - T_{i+\frac{1}{2}}|\Lambda|_{i+\frac{1}{2}}T^{-1}_{i+\frac{1}{2}}(Q_R - Q_L)\right] \tag{2.3.9}$$

with L and R representing the left and right states of the cell interface, respectively, and $|\Lambda|$ means taking the absolute value of each eigenvalue of the diagonal eigenvalue matrix, namely, $|\Lambda|_{i,i} = |\lambda_{i,i}|$.

The Roe average matrix $|A|_{i+\frac{1}{2}} = T_{i+\frac{1}{2}}|\Lambda|_{i+\frac{1}{2}}T^{-1}_{i+\frac{1}{2}}$ may be obtained by using the original matrix $A$ from Equation (2.1.6) and replacing it's components with Roe's averages defined by

$$\begin{aligned} u_{i+\frac{1}{2}} &= \frac{u_R\sqrt{\rho_R} + u_L\sqrt{\rho_L}}{\sqrt{\rho_R} + \sqrt{\rho_L}} \\ H_{i+\frac{1}{2}} &= \frac{H_R\sqrt{\rho_R} + H_L\sqrt{\rho_L}}{\sqrt{\rho_R} + \sqrt{\rho_L}} \end{aligned} \tag{2.3.10}$$

The speed of sound at the interface can be evaluated by

$$a_{i+\frac{1}{2}} = \sqrt{(\gamma - 1)(H_{i+\frac{1}{2}} - \frac{1}{2}u^2_{i+\frac{1}{2}})} \tag{2.3.11}$$

Assuming a frozen Roe matrix [1], the implicit operator may be written as

$$\begin{aligned} \frac{\partial R^k_i}{\partial Q_{i-1}} &= -\frac{1}{2\Delta x}\left(A_{i-1} + |A|_{i-\frac{1}{2}}\right) \\ \frac{\partial R^k_i}{\partial Q_i} &= \frac{1}{2\Delta x}\left(|A|_{i-\frac{1}{2}} + |A|_{i+\frac{1}{2}}\right) \\ \frac{\partial R^k_i}{\partial Q_{i+1}} &= \frac{1}{2\Delta x}\left(A_{i+1} - |A|_{i+\frac{1}{2}}\right) \end{aligned} \tag{2.3.12}$$

Note that it is assumed that $L = i$ and $R = i+1$ for the implicit operator. This does not affect the accuracy of the scheme as it is only assumed for the implicit part of the equation.

### 2.3.2 Positivity Preserving Scheme (CDF+)

A new positivity-preserving dual-time stepping scheme (referred to as CDF+ scheme) is presented [5]. This scheme guarantees positivity of the primitive variables by altering the eigenvalues of the Jacobian flux matrix.

Using the same discretization as the BDF1 scheme 2.3.2, the flux at the cell interface may be written using a flux vector splitting form (see [4] for details), namely,

$$E_{i+\frac{1}{2}} = T_i\Lambda^+_i T^{-1}_i Q_i + T_{i+1}\Lambda^-_{i+1}T^{-1}_{i+1}Q_{i+1} \tag{2.3.13}$$

For flux difference splitting with reconstruction–evolution, such as a fifth order WENO (see Section 2.3.3), the speed waves $[V_i^+], [V_{i+1}^-]$ take the form

$$[V_i^+]_{r,r} = \frac{1}{2\left[T_i^{-1}Q_i\right]_r}\left\{T_i^{-1} + \left[E_L + T_{i+\frac{1}{2}}\left(|A|_{i+\frac{1}{2}} - |\Lambda^{xt}|_{i+\frac{1}{2}}\Delta^{xt}_{i+\frac{1}{2}}\right)T^{-1}_{i+\frac{1}{2}}Q_L\right]\right\}_r - \frac{1}{2}\left[\Lambda^{xt}_L\Delta^{xt}_{i+\frac{1}{2}}\right]_{r,r} \tag{2.3.14}$$

$$[V_{i+1}^-]_{r,r} = \frac{1}{2\left[T_{i+1}^{-1}Q_{i+1}\right]_r}\left\{T_{i+1}^{-1} - \left[E_R + T_{i+\frac{1}{2}}\left(|A|_{i+\frac{1}{2}} - |\Lambda^{xt}|_{i+\frac{1}{2}}\Delta^{xt}_{i+\frac{1}{2}}\right)T^{-1}_{i+\frac{1}{2}}Q_R\right]\right\}_r - \frac{1}{2}\left[\Lambda^{xt}_R\Delta^{xt}_{i+\frac{1}{2}}\right]_{r,r} \tag{2.3.15}$$

The subscript r denotes the r$^{\text{th}}$ row of a vector, while the subscript $r, r$ denotes the r$^{\text{th}}$ element of a diagonal matrix.

The space-time eigenvalues are set to:

$$\left[\Lambda^{xt}\right]_{r,r} = \frac{[\Lambda]_{r,r}}{\max\left(1, \frac{\Delta t}{\Delta x}|\Lambda|_{r,r}\right)} \tag{2.3.16}$$

And the spacetime gradients are defined as:

$$\left[\Delta^{xt}_{i+\frac{1}{2}}\right]_{r,r} = \psi\left(\frac{\left[T_i^{-1}(Q_i - Q_i^n)\right]_r}{2[T_i^{-1}Q_i]_r}, \frac{\left[T_{i+1}^{-1}(Q_{i+1} - Q_{i+1}^n)\right]_r}{2[T_{i+1}^{-1}Q_{i+1}]_r}\right) \tag{2.3.17}$$

where

$$\psi(a,b) = \text{minmod}(a,b)\cdot\min\left(1, \xi\frac{\max(|a|,|b|)}{\min(|a|,|b|)}\right) \tag{2.3.18}$$

where the minmod function returns the argument that has the lowest magnitude if both arguments have the same sign and zero otherwise. Also, $\xi$ is a user-adjustable parameter, typically set to $\xi = 0.5$. Note that setting $[\Delta_{xt}]_{r,r} = 0$ would yield exactly the original Roe scheme.

Finally, the matrices $\Lambda_i^+$ , $\Lambda_{i+1}^-$ are given by:

$$\left[\Lambda_i^+\right]_{r,r} = \max\left(0, [V_i^+]_{r,r}\right) + \max\left(0, [V_{i+1}^-]_{r,r}\right) \tag{2.3.19}$$

$$\left[\Lambda_{i+1}^-\right]_{r,r} = \min\left(0, [V_i^+]_{r,r}\right) + \min\left(0, [V_{i+1}^-]_{r,r}\right) \tag{2.3.20}$$

Splitting the wave speeds between the left and right nodes such that $\Lambda_i^+$ has strictly positive elements and $\Lambda_{i+1}^-$ has strictly negative elements guarantees a positivity-preserving scheme.

In this scheme the implicit operator may be written as:

$$\frac{\partial R_i^k}{\partial Q_{i-1}} = -\frac{1}{\Delta x}\left(T_{i-1}\Lambda_{i-1}^+T_{i-1}^{-1}\right) \tag{2.3.21}$$

$$\frac{\partial R_i^k}{\partial Q_i} = \frac{1}{\Delta x}\left(T_i\Lambda_i^+T_i^{-1} - T_i\Lambda_i^-T_i^{-1}\right) = \frac{1}{\Delta x}T_i(\Lambda_i^+ - \Lambda_i^-)T_i^{-1} \tag{2.3.22}$$

$$\frac{\partial R_i^k}{\partial Q_{i+1}} = \frac{1}{\Delta x}\left(T_{i+1}\Lambda_{i+1}^-T_{i+1}^{-1}\right) \tag{2.3.23}$$

Although this scheme may appear as first order accurate in time, the added space-time terms to the flux, increase the order of the scheme to be between 1 and 2;

To prevent the appearance of carbuncle phenomena or other non-physical phenomena, it is necessary to condition the eigenvalue matrices $\Lambda^{\pm}$ appearing in the fluxes outlined in equations (2.3.19) and (2.3.20), as follows:

$$\begin{aligned}
\left[\Lambda_i^+\right]_{r,r} &\longrightarrow \min\left(q_{ref}+\frac{a_{ref}}{\zeta_2}, \left[\Lambda_i^+\right]_{r,r}\right)+\zeta_1(q_{ref}+a_{ref})\frac{P_{max}-P_{min}}{P_{min}} \\
\left[\Lambda_{i+1}^-\right]_{r,r} &\longrightarrow \max\left(-q_{ref}-\frac{a_{ref}}{\zeta_2}, \left[\Lambda_{i+1}^-\right]_{r,r}\right)-\zeta_1(q_{ref}+a_{ref})\frac{P_{max}-P_{min}}{P_{min}}
\end{aligned} \tag{2.3.24}$$

where $q_{ref}$ is a reference flow speed set to the maximum of the flow speeds at the nodes left and right of the interface and $a_{ref}$ is a reference sound speed set to the maximum of the sound speeds at the nodes left and right of the interface. As well, $P_{min}$ and $P_{max}$ are the minimum and maximum pressure on all nodes neighboring the interface. The user-adjustable parameter $\zeta_1$ is typically set between 0 and 0.3 while $\zeta_2$ is typically set between 0.1 and 0.5. Because the dissipation added is proportional to

$$\frac{P_{max}-P_{min}}{P_{min}}$$

and because the latter is only significant within 2 or 3 nodes of shock-waves, there is essentially no dissipation added in flow regions that are distant from shocks by 3 nodes or more. Thus, the latter eigenvalue conditioning affects the solution negligibly away from shocks. And last, the CDF+ scheme is more efficient memory wise than the BDF2 scheme, it only requires to store 2 time levels of the solution, similar to the BDF1 scheme.

### 2.3.3 Fifth Order WENO

In order to estimate the left and right states at every cell interface, a fifth-order WENO reconstruction scheme may be used [3]. Here the primitive variables $(\rho, u, p)$ are interpolated to the grid half-nodes using the WENO scheme. The fifth-order left and right interpolated variables are then written as

$$q_L = w_0^L q^{L_0} + w_1^L q^{L_1} + w_2^L q^{L_2} \tag{2.3.25}$$

$$q_R = w_0^R q^{R_0} + w_1^R q^{R_1} + w_2^R q^{R_2} \tag{2.3.26}$$

where

$$\begin{aligned}
q^{L_0} &= \frac{1}{3}q_{i-2} - \frac{7}{6}q_{i-1} + \frac{11}{6}q_i \\
q^{L_1} &= -\frac{1}{6}q_{i-1} + \frac{5}{6}q_i + \frac{1}{3}q_{i+1} \\
q^{L_2} &= \frac{1}{3}q_{i-1} + \frac{5}{6}q_i - \frac{1}{6}q_{i+1}
\end{aligned} \tag{2.3.27}$$

$$\begin{aligned}
q^{R_0} &= \frac{1}{3}q_{i+3} - \frac{7}{6}q_{i+2} + \frac{11}{6}q_{i+1} \\
q^{R_1} &= -\frac{1}{6}q_{i+2} + \frac{5}{6}q_{i+1} + \frac{1}{3}q_i \\
q^{R_2} &= \frac{1}{3}q_{i+1} + \frac{5}{6}q_i - \frac{1}{6}q_{i-1}
\end{aligned} \tag{2.3.28}$$

The smoothness indicators for the left and right states are given by

$$\begin{aligned}
\beta_0^L &= \frac{12}{13}\left(q_{i-2} - 2q_{i-1} + q_i\right)^2 + \frac{1}{4}\left(q_{i-2} - 4q_{i-1} + 3q_i\right)^2 \\
\beta_1^L &= \frac{12}{13}\left(q_{i-1} - 2q_i + q_{i+1}\right)^2 + \frac{1}{4}\left(q_{i+1} - q_{i-1}\right)^2 \\
\beta_2^L &= \frac{12}{13}\left(q_i - 2q_{i+1} + q_{i+2}\right)^2 + \frac{1}{4}\left(3q_i - 4q_{i+1} + q_{i+2}\right)^2
\end{aligned} \tag{2.3.29}$$

$$\begin{aligned}
\beta_0^R &= \frac{12}{13}\left(q_{i+3} - 2q_{i+2} + q_{i+1}\right)^2 + \frac{1}{4}\left(q_{i+3} - 4q_{i+2} + 3q_{i+1}\right)^2 \\
\beta_1^R &= \frac{12}{13}\left(q_{i+2} - 2q_{i+1} + q_i\right)^2 + \frac{1}{4}\left(q_{i+2} - q_i\right)^2 \\
\beta_2^R &= \frac{12}{13}\left(q_{i+1} - 2q_i + q_{i-1}\right)^2 + \frac{1}{4}\left(3q_{i+1} - 4q_i + q_{i-1}\right)^2
\end{aligned} \tag{2.3.30}$$

The modified weights are given by

$$\tilde{w}_k = \frac{\gamma_k}{(\varepsilon + \beta_k)^2} \tag{2.3.31}$$

The term $\varepsilon$ is a small number to avoid division by zero. The optimal weights $\gamma_0$, $\gamma_1$, and $\gamma_2$ for fifth-order in space are given as 0.1, 0.6, and 0.3, respectively. Finally, the modified weights are renormalized by

$$w_k = \frac{\tilde{w}_k}{\sum_{j=0}^{2} \tilde{w}_j} \tag{2.3.32}$$

# Chapter 3

# Sod Test Case

The Sod case, named after Gary A. Sod, is a common test case to test the accuracy of CFD schemes. The test consists of a 1-D shock tube with two different states that are separated completely from each other in the middle of the tube. At $t = 0$ $[sec]$ the separation between the two states disappears. The different pressure between the two states causes a shock wave, an expansion fan, and a contact discontinuity to form and propagate throughout the tube.

The initial conditions are such that the fluid starts at rest, the pressure is set to $10kPa$ and $100kPa$ for the left and right states, respectively, and the density is set to 0.1 $[\frac{kg}{m^3}]$ within both states. This particular problem is chosen as a sort of a difficult stress test for dual-time stepping schemes as will become evident by the results. The tube length is set to $L = 1.2$ $[m]$ and the number of nodes is set to 481.

Figures 3.1 and 3.2 show the density and temperature profiles using a relativity small time step of $\Delta t = 1$ $[\mu s]$. The difference between the results is very small, showing that the CDF+ scheme is as accurate as the original BDF2 scheme. The CDF+ scheme is somewhat more diffusive, resulting from the alteration of the eigenvalues of the Jacobian matrix, but generally the results are practically identical.

Figure 3.3 shows the density profile while using a larger time step of $\Delta t = 5$ $[\mu s]$. While the regular BDF2 scheme exhibits large oscillation at the discontinuities, the CFD+ scheme remains monotone with no non-physical oscillations. This provides a clear evidence that the CDF+ scheme is more stable for large time steps.

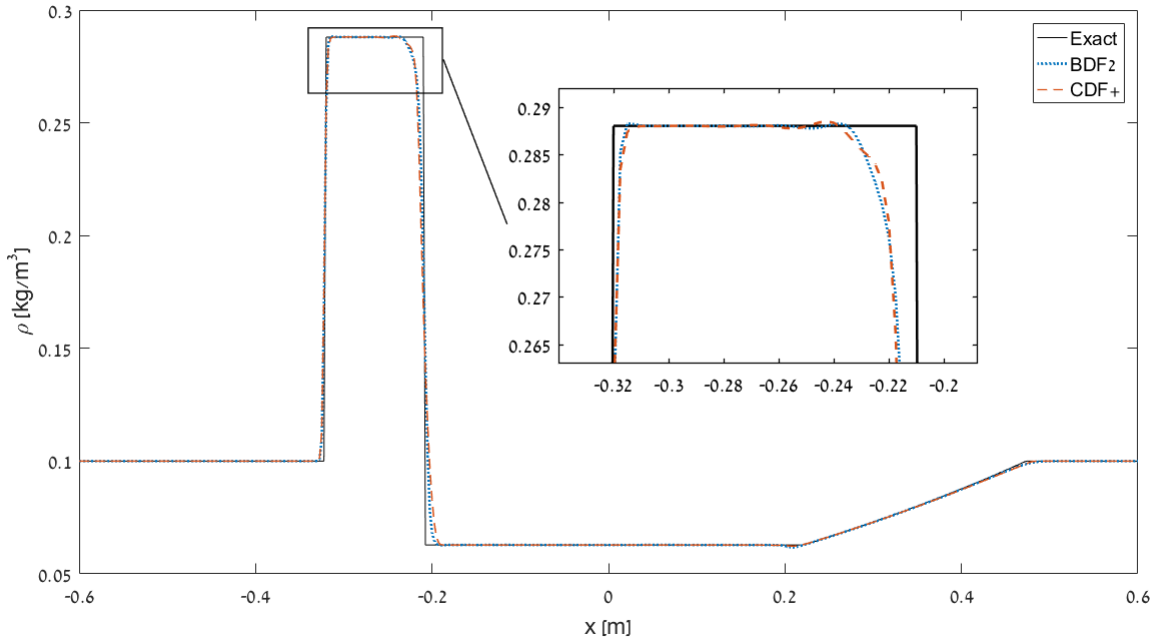


Figure 3.1: Density profile at $t = 0.4ms$, $\Delta t = 1$ $[\mu s]$

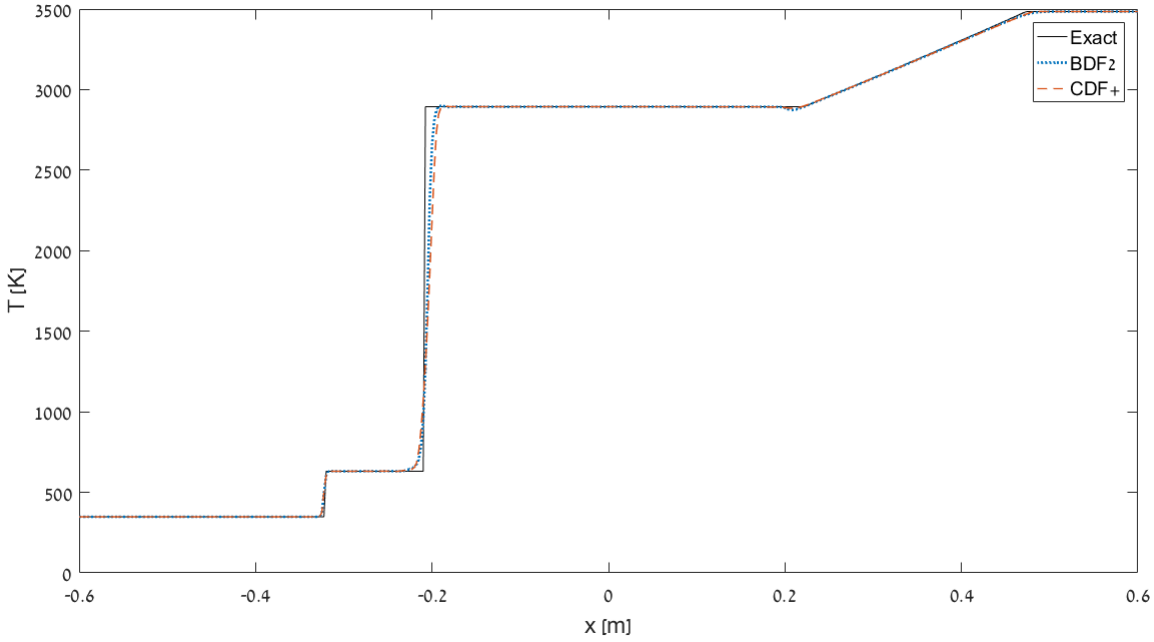


Figure 3.2: Temperature profile at $t = 0.4ms$, $\Delta t = 1$ $[\mu s]$

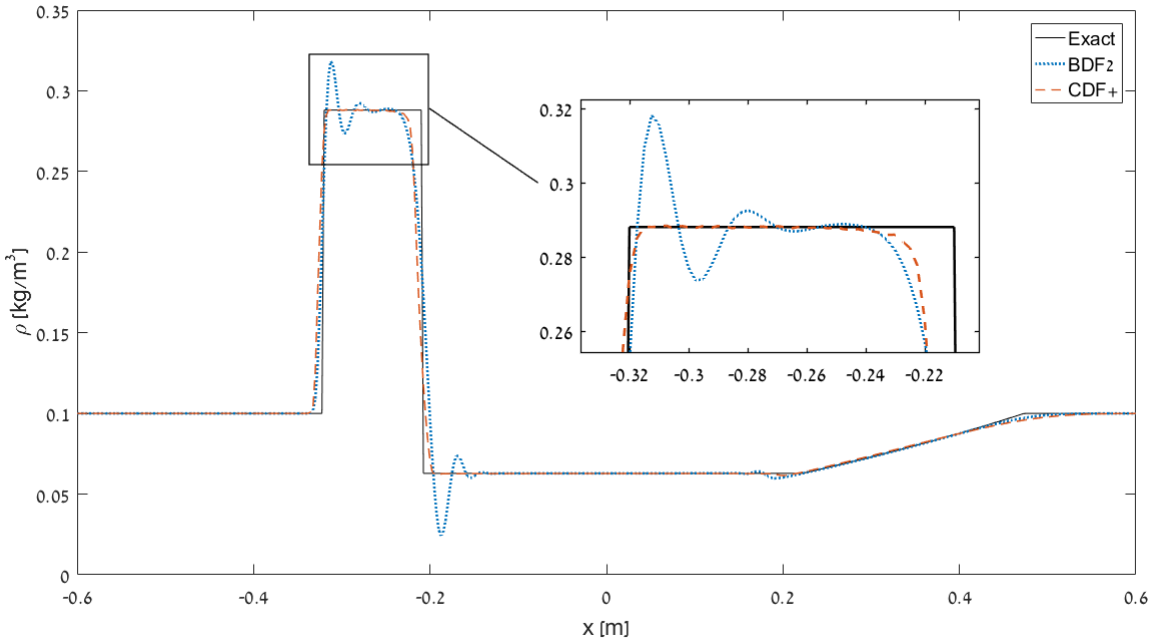


Figure 3.3: Density profile at $t = 0.4ms$, $\Delta t = 5$ $[\mu s]$

| Scheme | $\Delta t = 1$ $[\mu s]$ | | $\Delta t = 5$ $[\mu s]$ | |
|---|---|---|---|---|
| - | Density error | Temperature error | Density error | Temperature error |
| BDF2 | 0.0071 | 0.0077 | 0.0304 | 0.0247 |
| CFD+ | 0.0093 | 0.0101 | 0.0164 | 0.0119 |

Table 3.1: Relative error of each scheme using different time steps

Table 3.1 shows the relative error of each scheme using various time steps. The error was calculated using the following formulae

$$T_{error} = \frac{1}{L} \int_{-\frac{L}{2}}^{\frac{L}{2}} \left| \frac{T - T_{exact}}{T} \right| dx \tag{3.0.1}$$

$$\rho_{error} = \frac{1}{L} \int_{-\frac{L}{2}}^{\frac{L}{2}} \left| \frac{\rho - \rho_{exact}}{\rho} \right| dx \tag{3.0.2}$$

As is evident from the figures, the BDF2 scheme is slightly more accurate when using a small time step but significantly less accurate for larger time steps.

# Chapter 4

# Conclusion

A new positivity preserving scheme for the Euler equation that can be used with dual-time stepping was tested. The scheme, named CDF+, alters the eigenvalues of the Jacobian matrix to guarantee that all the primitive variables remain positive throughout the solution. The scheme also guarantees that the solution remains monotone near discontinuities, a property that was shown using the Sod test case.

When using a small time step, the CDF+ scheme and the BDF2 scheme behave practically the same, showing that the new scheme captures the solution with high accuracy. When using a large time step, the use of the standard BDF2 scheme results in large oscillations near discontinuities while the CDF+ scheme maintains monotonicity as it entirely eliminates any oscillations. The new scheme is also more efficient memory wise. While high order methods such as the BDF2 scheme require to store the solution for multiple time levels, the CDF+ scheme only requires to store 2 time levels of the solution, similar to the BDF1 scheme.

# References


[1] Jiri Blazek. *Computational fluid dynamics: principles and applications*. Butterworth-Heinemann, 2015.

[2] Joel H Ferziger and Milovan Peric. *Computational methods for fluid dynamics*. Springer Science & Business Media, 2012.

[3] Robert H Nichols, Robert W Tramel, and Pieter G Buning. Evaluation of two high-order weighted essentially nonoscillatory schemes. *AIAA journal*, 46(12):3090–3102, 2008.

[4] Bernard Parent. Positivity-preserving flux difference splitting schemes. *Journal of Computational Physics*, 243:194–209, 2013.

[5] Bernard Parent. Positivity-preserving dual time stepping schemes for gas dynamics. *Journal of Computational Physics*, 361:391–411, 2018.

[6] Philip L Roe. Approximate riemann solvers, parameter vectors, and difference schemes. *Journal of computational physics*, 43(2):357–372, 1981.